226 (2023) 211759

Contents lists available at ScienceDirect

Geoenergy Science and Engineering

journal homepage: www.sciencedirect.com/journal/geoenergy-science-and-engineering

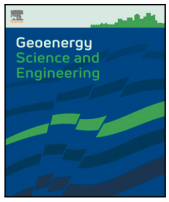

Energy efficiency of oil and gas production plant operations

Handita Reksi Dwitantra Sutoyo [a,*], I Gusti Agung Gede Angga [a], Heiner Schümann [b], Carl Fredrik Berg [a]

[a] Department of Geoscience and Petroleum, Norwegian University of Science and Technology, S.P. Andersens veg 15, Trondheim, 7031, Norway
[b] Department of Process Technology, SINTEF Industry, Tillerbruvegen 200, Trondheim, 7092, Norway

ARTICLE INFO

Keywords:
Energy efficient
Processing plant
Gas compression
Pumping
Optimization

ABSTRACT

The exploitation of subsurface resources is an energy-intensive activity leading to substantial emissions. The main energy consumer for hydrocarbon production is gas compression and pumping. In this article, we investigate the effect on energy use from changes to compressor and pump layout, with a particular focus on offshore platforms. We have developed a workflow for the optimization of compressor and pump layout and settings, where the optimization objective is the minimization of energy use. The introduced workflow is demonstrated on simulated data from an offshore field. We first compared how the interval between operational changes to the processing plant affects energy use and observed significant reductions in energy use when increasing the number of operational changes, e.g., a 7% reduction when moving from quarterly to monthly changes and an additional 5% reduction when moving to weekly changes. However, the reductions diminish with an increasing number of operational changes. This indicates that more sophisticated processes such as fully automatic operations to change the setup continuously are not a necessity for efficient operations, considering practical and operational limitations to changes in equipment layout. Increasing the degrees of freedom by allowing for changes to the rotational speed, both for compressors and pumps, yields an additional reduction in energy use, thereby reducing associated emissions. The increased flexibility of changes to the rotational speed gave an energy reduction of 9% on average for our test case. In addition, our study shows a strong correlation between energy efficiency and the amount of gas needed to prevent surge in the compressors.

1. Introduction

The oil and gas sector has played a dominant role in fulfilling energy demand for the past decades. Although the Covid-19 pandemic temporarily reduced oil consumption due to movement and travel restrictions, oil consumption started to bounce back in 2021. On the other hand, natural gas remains a major resource for electricity production worldwide. It has been projected that gas will continue as a major portion of the global energy mix until 2050 (IEA, 2021a). A production decline of hydrocarbons will create a gap between supply and demand. There are many challenges to face off a possible supply–demand gap, including technological advancement to recover reducing resources, and increasing operational and environmental costs of production (IEA, 2022; Aguilera, 2021; Al-Fattah, 2020). Besides the emissions associated with the consumption of the product, e.g., burning in combustion engines, the oil and gas production process itself is a large contributor to CO_2 emissions. In Norway, as an example, CO_2 emissions from the oil and gas sector account for 25% of Norway's total emissions, corresponding to 13.2 million tonnes (Sentralbyrå, 2021). These emissions are associated with power generation on the offshore platforms, accounting for 85% of emissions, followed by support and transport, where combustion engines account for less than 10% of the total emissions from the oil and gas industry. To reduce emissions, the Norwegian government introduced CO_2 taxes in 1991, which are expected to reach a rate of 2000 NOK/ton CO_2 (approximately 200 \$/ton CO_2) by 2030 (NPD, 2021). To meet the increased penalty cost of emissions from CO_2 taxes, major operators are developing new production strategies, implementing new low carbon emission technologies, and introducing renewable methods for power generation (IEA, 2021b).

Power consumption and emissions are different for each platform and vary strongly during the lifetime of a field. Total power consumption depends on the field characteristics (fluid type, production rate), export specifications (sales points, specifications, pressure, and temperature), field lifetime, etc. Bothamley (2004). Injection systems for pressure support, oil export pumping systems, and gas compression are the primary consumers of power in the processing plant. If oil is

* Corresponding author.
E-mail addresses: handita.r.d.sutoyo@ntnu.no (H.R.D. Sutoyo), i.g.a.g.angga@ntnu.no (I.G.A.G. Angga), heiner.schumann@sintef.no (H. Schümann), carl.f.berg@ntnu.no (C.F. Berg).

https://doi.org/10.1016/j.geoen.2023.211759
Received 18 January 2023; Received in revised form 27 February 2023; Accepted 31 March 2023
Available online 5 April 2023

offloaded to tank ships directly at the platform, the energy consumption of oil pumping is a minor part of the total power consumption at the platform (with corresponding emissions from the transport ships). However, when the produced oil is transported in export pipelines to refineries onshore, the energy consumption is significant. Water flooding is a widely used method to increase production, and pumping water into the reservoir is typically a significant source of power consumption. Ultimately, we have a gas compression system that is utilized to increase the gas's pressure for gas lift, gas injection, or export as sales gas transported through pipes. Overall, the gas compression system can consume up to 50% of the total available power of the platform, depending on the amount of gas in the whole production system (Nguyen et al., 2013).

The first measure to reduce emissions associated with gas compression is by reducing the related power consumption in the processing plant. Nguyen et al. (2016) highlights several possibilities for reducing the power consumption in the processing plant, e.g., increasing the efficiency of the equipment and changing the production strategy to reduce power consumption, which will be unique for different fields. With varying demands on flow rate and head along the lifetime, increased efficiency can be obtained by replacing equipment with more suitable sizing for certain periods. For low production rates in the late life of a field, pumps, and compressors typically operate far off their designed rate and replacing them could yield significant efficiency gains. Specifically for the compressors, more optimal sizing will reduce the need of using anti-surge methods to protect the compressors, thereby increasing efficiency (Nguyen et al., 2014; Voldsund et al., 2013; Arun Shankar et al., 2016).

Another measure for emission reduction is to increase the efficiency of the power generation system. Nguyen et al. (2014) showed that the turbine system itself is part of the power generating system with the lowest efficiency. Several studies show how to increase gas turbine efficiency. One study for the Oseberg and Snorre fields on the Norwegian Continental Shelf (NCS) investigated a cogeneration plant with a steam cycle. However, the installation had several challenges concerning weight and space constraints for the platform (Kloster, 1999, 2000). An integrated concept of increasing power generation efficiency by integrating gas turbine, waste heat recovery unit, steam cycle, and power from shore was studied by Riboldi and Nord (2017). It showed that electrification from the shore reduced emissions up to 35.5%, while a combined cycle gave a reduction of 32.2%.

Several studies have compared the cost of installing a new power supply system with continued use of the current gas turbine installations (McKenna et al., 2021; Zhong and Bazilian, 2018). As expected, continued use of the current gas turbine installations yields a lower cost of electricity generation compared to installing a power supply based on energy sources with lower emissions. Similar observations were made for electrification from shore; while the long-term costs are promising, such installations face high investment costs (Roussanaly et al., 2019).

The aforementioned studies indicate that for existing platforms with a limited remaining lifetime, a promising emission reduction strategy is to optimize the processing plant power consumption and, thereby, emissions. This study presents a methodology and workflow for reducing the power consumption from oil and gas processing plants, resulting in CO_2 emission reductions. The focus will be on reducing power consumption based on the existing capabilities of the processing plant and its equipment by operating the processing plant more flexibly. The contributions of this paper can be summarized as follows:

- This work presents a general workflow applicable to any field with a (possibly historical) performance test of the equipment. Performance tests are utilized to model the equipment, and these models are employed in the model of the processing plant based on actual equipment. The objective of the optimization is to reduce power consumption, thereby reducing emissions associated with oil and gas production.
- Using the reservoir fluid going to the processing plant (inlet) and fluid to be discharged from it (outlet), we can calculate the required capacity of the processing plant, and translate these requirements into optimal configurations and operational settings. This paper will compare operational flexibility by comparing the effect of different time intervals between interventions to change the operational configurations and settings of the processing plant.

Table 1
Required data for modeling of the processing plant efficiency. Parameters marked with an asterisk, *, can vary depending on the operational constraints of the processing plant and field lifetime. E.g., changing the inlet pressure and outlet pressure of the separator will affect the first stage compressor inlet.

Parameter	Value	
Oil production rate	$q_{op}(t)$	From field profile
Water production rate	$q_{wp}(t)$	From field profile
Gas production rate	$q_{gp}(t)$	From field profile
Water injection rate	$q_{wi}(t)$	From field profile
Gas injection rate	$q_{gi}(t)$	From field profile
Processing plant inlet pressure	p_m *	20×10^5 Pa
First stage compressor inlet	p_{ic} *	5×10^5 Pa
Separator output pressure	p_p *	5×10^5 Pa
Gas export pressure	p_d *	200×10^5 Pa
Gas injection pressure	$p_{gi}(t)$	From field profile
Water injection pressure	$p_{wi}(t)$	From field profile

While previous studies have focused on the effect of installing new equipment, this study offers a solution to reduce power consumption that can be implemented directly without installing new, removing or modifying the current equipment, thereby unlocking opportunities for emission reductions without time delay for implementation and spending for additional investment.

This paper is structured as follows. Section 2 will cover the methodology and approach used for this study; this includes assumptions, processing plant modeling and optimization, and the overall workflow for estimating power consumption from different strategies. Section 3 presents a case study for our developed methodology. Section 4 discusses the results from the case study, while Section 5 summarizes this study and its consequences.

2. Methodology

This section will describe the methodology and workflow presented in this paper. It starts by describing the required data (Section 2.1), followed by the modeling of the process plant (Section 2.2), and finally the optimization of the processing plant (Section 2.3).

2.1. Input data

This paper requires several types of input data to calculate the power consumption for different configurations of the pump and compressor system. The required input data are summarized as follows:

- Flow rates and pressures of fluids entering the processing plant. These are fluids produced from the reservoir, consisting of oil production, water production, and gas production.
- Flow rates and pressures of fluids leaving the processing plant as injection fluids. This will determine the required power to inject fluids (e.g., water for pressure support) into the reservoir.
- Pressures of fluids leaving the processing plant for export through export lines. The rates can be inferred from the difference between production and re-injection.

A summary of the required input values for this study is shown in Table 1. The case study will use simulated production and injection profiles from the Norne field (OPM, 2022), an offshore field in the North Sea, which has water injection and gas injection facilities. In addition, the remaining gas after re-injection will be exported to onshore facilities at a constant export pressure.

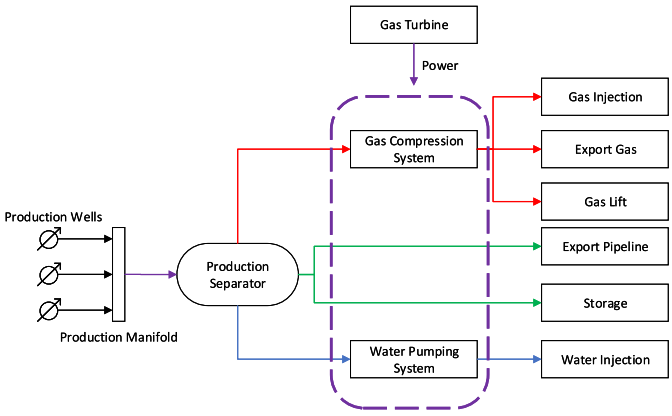

Fig. 1. Illustration of a typical layout of a processing plant on an offshore platform. This study assumes that the oil production goes directly into storage, with no power required for this operation.

2.2. Modeling of the processing plant

The processing plant on an offshore platform often contains gas turbines, gas compressors, and pumps as main power consumer units. Fig. 1 shows a typical layout of these three components within a processing plant (Bothamley, 2004). Other standard components are separators, heaters/heat exchangers, water treatment systems, scrubbers, etc. As these other components are assumed to consume less energy (Nguyen and de Oliveira Júnior, 2018), we consider them secondary concerning minimizing energy consumption. However, the workflow proposed in this article can be extended to include other components, with an associated increase in modeling complexity and computational cost.

The methodology presented in this paper relies on several assumptions:

- The reservoir production data is obtained from a black oil reservoir simulation model. The black oil model has constant surface composition for both oil and gas.
- This study uses a single-stage separation process, as shown in Fig. 2(b), instead of multi-stage separation in the processing plant. Fig. 2(a) shows a more realistic separation process in the processing plant, which includes re-compression of separated gas in each stage. The conclusions drawn from this study are assumed unaffected by the choice of separation model. To reduce complexity and computational cost we use the single-stage separation model.
- We model a steady-state process for each time step. Any transient phenomena and related consequences for the processing plant are not investigated in this study.

As mentioned, we focus on the water pumping and gas compression systems, as these consume most of the power on typical offshore platforms. We will model the pumping and gas compression system using an analytical model based on a realistic number of compressors and pumps for an offshore platform (Bothamley, 2004).

2.2.1. Pump modeling

Water is injected into the reservoir to sweep out oil and for pressure support. Fluctuation in injection rate and pressure may result in inefficient pumping operations. Pumps in older facilities might be single-speed, while newer facilities can have variable-speed pumps that can operate more efficiently at different rates and pressures. Still, a proper design and control of the pumping system, depending on the injection requirements, will increase its efficiency (Arun Shankar et al., 2016; Viholainen et al., 2013).

In this study, we consider a pumping system with a specified number of stages (n) and trains (m), as shown in Fig. 3. The pumping system consists of individual pumps, where all pumps are assumed to be running with the same rotational speed and have identical performance. The pump performance is derived from functional relationships where the head difference (h_p) and efficiency (η_p) are described as functions of the volumetric rate of fluid flow entering the pump (q_p) and the rotational speed of the pump (ω_p) (Stewart, 2019a):

$$h_p = h_p(q_p, \omega_p) \tag{1}$$

$$\eta_p = \eta_p(q_p, \omega_p) \tag{2}$$

These functions are described in detail in Appendix B. The same appendix contains pump-specific constants as used in this study. From the head, efficiency, and flow rate we can compute the required power consumption of the pump (P_p) as (Stewart, 2019a):

$$P_p = \frac{q_p \cdot \rho_f \cdot g \cdot h_p}{\eta_p} \tag{3}$$

where ρ_f is the density of the fluid flowing in the pump, and g is the gravitational acceleration.

For the combined pumping system consisting of m trains with n stages, let $p_{i,j}$ represent the pump at train i and stage j. The combined pumping system will then have a total head difference, h_{ps}, total pumping rate, q_{ps}, and total power consumption, P_{ps}, formulated as:

$$h_{ps} = \sum_{j=1}^{n} h_{p_{i,j}} \tag{4}$$

$$q_{ps} = \sum_{i=1}^{m} q_{p_{i,j}} \tag{5}$$

$$P_{ps} = \sum_{i,j=1}^{n,m} P_{p_{i,j}} \tag{6}$$

Here the summation for the total head can be for any given train $i \in [1, m]$, while the summation for the total rate can be for any given stage $j \in [1, n]$. With equal pump performance curves and a single rotational speed all rates $q_{p_{i,j}}$ will be equal, while for a given stage j the head drop $h_{p_{i,j}}$ will be equal for each train i. The total power consumption P_{ps} will be part of the objective for optimization, later used in Eq. (15).

2.2.2. Compressor modeling

A centrifugal compressor is the most common type of compressor used in processing plants due to its ability to handle a wide range of flow rates and compression ratios, and at the same time, it is found to be easy and cheap to maintain Stewart (2019b). Similar to the pump performance, the compressor performance is derived from functional relationships where the pressure ratio (p_r) between the outlet discharge and inlet suction, and the isentropic efficiency (η_s) are described as functions of corrected mass flow rate ($\dot{m}_c$) and corrected rotational speed (ω_c):

$$p_r = p_r(\dot{m}_c, \omega_c) \tag{7}$$

$$\eta_s = \eta_s(\dot{m}_c, \omega_c) \tag{8}$$

where corrected mass flow ($\dot{m}_c$) and corrected rotational speed (ω_c) are defined as:

$$\dot{m}_c = \dot{m} \cdot \sqrt{\frac{T_i}{T_{sc}}} \cdot \frac{p_{sc}}{p_i} \tag{9}$$

$$\omega_c = \omega \cdot \frac{T_{sc}}{T_i} \tag{10}$$

where $\dot{m}$ is the mass flow rate through compressor, ω is the rotational speed of the compressor, p_i is the inlet pressure condition of the compressor, p_{sc} is pressure in standard condition (1×10^5 Pa), T_i is

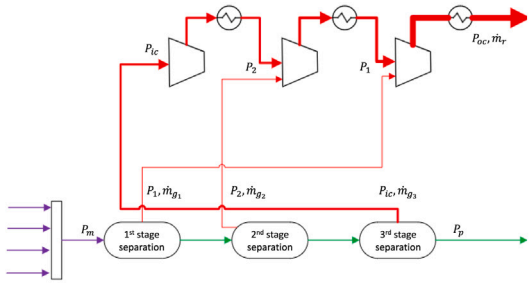

(a) Gas separator and compressor system with recompression scheme for a three stage system. Here P_{ic} is the pressure outlet of the last separation stage, and the inlet pressure of the first compression stage.

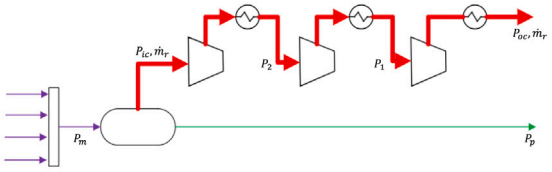

(b) Single stage separation process, with outlet pressure of the separation of P_{ic}, which is then the inlet pressure to the first stage of the compression system.

Fig. 2. Comparison of a (a) actual oil and gas separation system with several separation stages, with the simplified (b) single separation system assumed in this study.

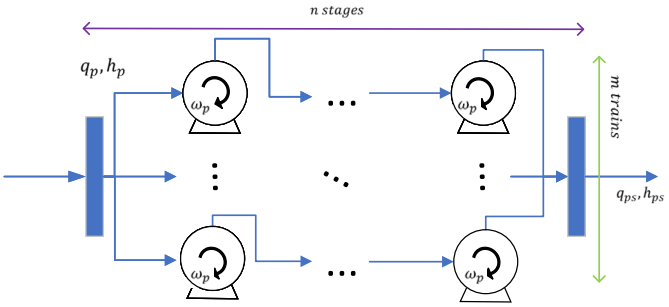

Fig. 3. Illustration of the pumping system with multiple stages (n) and trains (m) consisting of pumps operating at the same rotational speed ω_p.

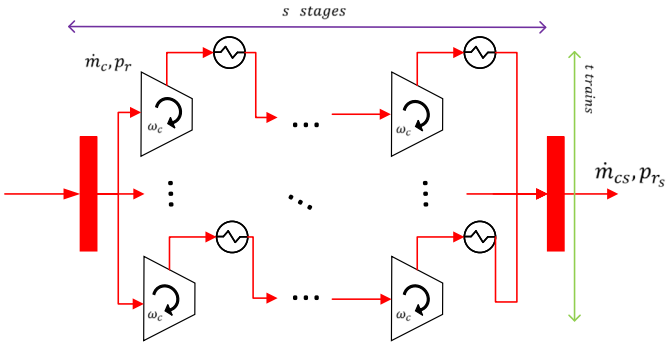

Fig. 4. Illustration of the compressor system model using multiple stages (s) and trains (t). After each compressor, the compressed gas will go through a heat exchanger and is assumed to be cooled down to the inlet temperature of T_i.

the inlet temperature, and T_{sc} is temperature in standard condition 273.15 K (Stewart, 2019b).

Several studies have modeled the compressor performance using analytical expressions for the pressure ratio and efficiency (Yazar et al., 2017; Shen et al., 2020; Jiang et al., 2019). Operational constraints for the compressor have also been described (Leufvén and Eriksson, 2013). In this study, we will use the compressor model of Jiang et al. (2019), presented in Appendix C. We will fit the two relationships p_r and η_s to data for a compressor assumed to be typical for offshore use at the NCS.

Based on the description for p_r and η_s, we can find the power consumption (P_c) of the compressor for certain mass flow and pressure ratio as (Stewart, 2019b):

$$P_c = \frac{\left(\frac{k}{k-1}\right) \cdot \dot{m} \cdot z \cdot R \cdot T \cdot \left(p_r^{\left(\frac{k-1}{k}\right)} - 1\right)}{\eta_s} \tag{11}$$

where k is the heat capacity of the gas, z is the compressibility factor of the gas, R is the gas constant, and T is the temperature.

We will assume a set of identical compressors. These identical compressors will form a compressor system consisting of several stages (s) and trains (t) and are assumed to be working at the same rotational speed of ω_c, as visualized in Fig. 4. At each compression stage, we assume that the compressed gas will go through a heat exchanger which will cool the gas back down to T_i. The compressor system will have a total pressure ratio, $p_{r_{cs}}$, corrected mass flow, $\dot{m}_{cs}$, and power consumption, P_{cs}, formulated as:

$$\dot{m}_{cs} = \sum_{i=1}^{t} \dot{m}_{c_{i,j}} \tag{12}$$

$$p_{r_{cs}} = \prod_{j=1}^{s} p_{r_{i,j}} \tag{13}$$

$$P_{cs} = \sum_{i,j=1}^{s,t} P_{c_{i,j}} \tag{14}$$

Here the summation over trains in Eq. (12) can be conducted for any stage j, and the product over stages in Eq. (13) can be conducted for any train i.

Both pumping and compressor systems have several operational limits. The following section will elaborate on optimizing the operation of the pumping and compression system by considering the equipment limits, performance, and boundary conditions as described before. Both possibilities of reducing power consumption by a simple online/offline schedule of the trains or stages, and a more flexible approach for reducing power by additionally adjusting the rotational speed, will be investigated below.

2.3. Optimization

As given by Eqs. (6) and (14), the power consumption of the processing plant for a given mass flow rate and pressure ratio depends on the pump and compressor setup. If the required mass flow rate and pressure ratio for a drainage scenario can be predicted, we can find the optimal pump and compressor setup to minimize the power consumption of the processing plant.

In this study, we will use reservoir simulations to predict the processing plant's requirements. Thus, each time step in the reservoir simulation yields a set of rates and pressures for the simulated drainage, and we need to find a processing plant setup that is optimal for the given requirements. The processing plant setup is defined by the number of trains and stages for the pumps and compressors. We assume that the facilities remain constant, thus we are limited by the maximal

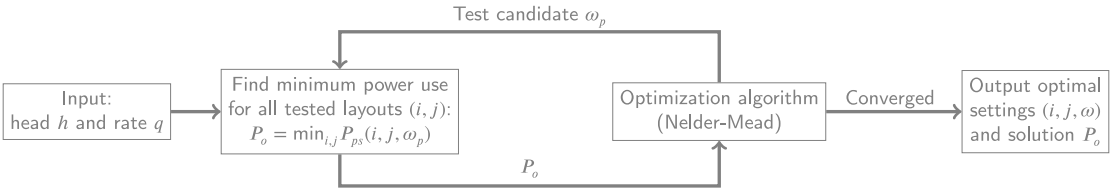

Fig. 5. A flowchart of the optimization loop with varying rotational speed ω. The flowchart when using only maximal rotational speed is similar but without the optimization loop. The compressor optimization described below is also similar.

number of trains and stages available at the platform. This means that the number of possible configurations is limited by the product of the maximum number of trains and stages. The relatively small number of possible setups allows for a brute-force approach to the optimization problem. We have tried using a population-based approach to the optimization problem, but this was significantly slower than the brute-force approach. Other authors have also reported long computational times for this optimization task when using population-based optimization techniques (Li et al., 2021).

In the brute-force approach, we find the lowest power consumption for all the possible configurations layouts and then chose the configuration yielding the lowest power consumption, as given by Eq. (6) and (14), as the optimal configuration.

2.3.1. Pump optimization

In this section, we will focus on the control of the pumping system operation (Arun Shankar et al., 2016). da Costa Bortoni et al. (2008) presented an optimization scenario where pumping system efficiency is limited by having an online–offline schedule, working on fixed rotational speed. Ahonen et al. (2019) expanded the possibility of changing rotational speed to increase the pumping system's efficiency. We will consider both cases.

For pump optimization, we assume an existing pumping system in the processing plant with a specified number of trains and stages. Further, the pumps have specified performance curves, with the performance curves used in this study given in Appendix B. We optimize the number of pumps in use, assuming that the remanding pumps are bypassed. In the optimization we assume that all trains have the same number of stages, thus we bypass the same number of pumps in each train. The objective function to be minimized in our problem is the total power consumption of the pumping system: P_{ps}. The optimization problem for the pumping system can then be formulated as follows:

$$\begin{aligned} \min_{i,j,\omega_p} \quad & P_{ps}(i,j,\omega_p) \\ \textbf{s.t.} \quad & 1 \le i \le n; \quad i \in \mathbb{Z} \\ & 1 \le j \le m; \quad j \in \mathbb{Z} \\ & \omega_{p_{min}} \le \omega_p \le \omega_{p_{max}}; \quad \omega_p \in \mathbb{R} \end{aligned} \tag{15}$$

where it fulfills the constrain of the required head (h_r) and rate (q_r):

$$h_{ps} \ge h_r$$
$$q_{ps} \ge q_r$$

Here the power P_{ps}, head h_{ps} and rate q_{ps} for the pumping system are given by Eqs. (4)–(6). This was optimized using brute force in the variables i and j, and Nelder–Mead for the rotational speed ω_p for each given pair of i and j values. If we optimize with respect to a fixed rotational speed, then we fix $\omega_p = \omega_{p_{max}}$. Fig. 5 shows a flowchart indicating the optimization workflow used in this study. A similar workflow will be used for the compressor system.

2.3.2. Compressor optimization

Compressor system optimization has been studied by several authors. As an example, studies on the use of a variation of guide vane and suction throttling are found to improve the efficiency (Kurz and Brun, 2017). Also, the use of Model Predictive Control (MPC), load sharing algorithms, and variable speed drive has been shown to enhance existing compressor system performance (Cortinovis et al., 2016; Milosavljevic et al., 2020; Paparella et al., 2013). This study implements the load-sharing framework and variation of rotational speed to increase efficiency. The objective function to be minimized is the total power consumption of the compressor system: P_{cs}. The optimization problem can then be formulated as follows:

$$\begin{aligned} \min_{i,j,\omega_c} \quad & P_{cs}(i,j,\omega_c) \\ \textbf{s.t.} \quad & 1 \le i \le s; \quad i \in \mathbb{Z} \\ & 1 \le j \le t; \quad j \in \mathbb{Z} \\ & \omega_{c_{min}} \le \omega_c \le \omega_{c_{max}}; \quad \omega_c \in \mathbb{R} \end{aligned} \tag{16}$$

bound with the constraints of the required mass flow by the system ($\dot{m}_{cs}$) and pressure ratio ($p_{r_{cs}}$):

$$p_{r_{cs}} \ge p_{r_r}$$
$$\dot{m}_{cs} \ge \dot{m}_r$$

As with the pumping system optimization, we also here use a brute-force approach in i and j, and Nelder–Mead for the rotational speed for each pair of i and j values. This approach is again efficient, as the different possible compressor system layouts are limited by the number of trains and stages, i.e., limited by $n \times m$, which is a relatively small number for a typical offshore compressor system.

3. Case study

In this section, we will test the workflow for obtaining optimum processing plant operations in a case study. Our case study is based on the reservoir simulation results from the Norne field in the Norwegian sea (OPM, 2022). This simulation model provides us with nine years of oil, gas, and water production and gas and water injection profiles. We extract these profiles, including the required discharge pressure from the processing plant for both gas and water injection, providing the required head (h_r) for the water injection system and the required pressure ratio (p_{r_r}) for the gas compression system. In addition, the gas compression system will also handle the gas export through a constant discharge pressure (p_d). As the gas compression system is delivering gas both to gas export and gas injection, the required discharge pressure from the gas compression system will be the maximum of the gas injection pressure and pressure needed for the export system.

The case study will inspect two main objectives to be explored in this study. First, we will compare the efficiency of adding an additional degree of freedom to the pumping and compressor system operations: As explained previously, we consider two different pump and compressor systems. The first one with a conservative way to operate the system has an online–offline schedule of the equipment and works with a maximum rotational speed. While for the second we will add rotational speed as another variable to operate the system. The second objective is to examine the impact of the frequency of changing the operation of the processing plants. We inspect different schedules for changing the configuration as elaborated in the following:

1. There is no change in the processing plant configuration. It means we define a single configuration throughout the nine years field profile, i.e., a fixed number of trains and stages, covering the highest requirements of the processing plant capacities.

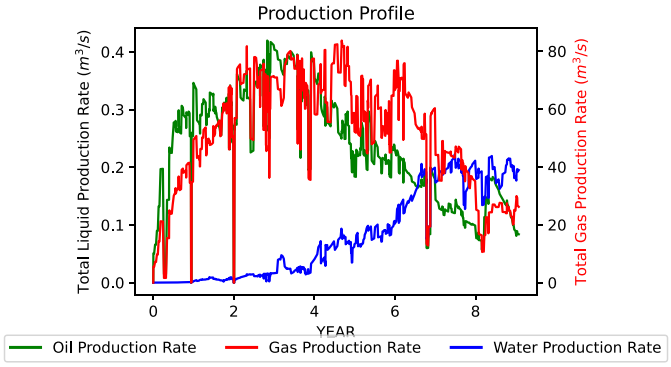

(a) Production profile for the Norne field. The liquid production rates are shown in the green and blue lines for oil and water production respectively. The gas production profile is shown with a solid red line, and corresponds to the right axis.

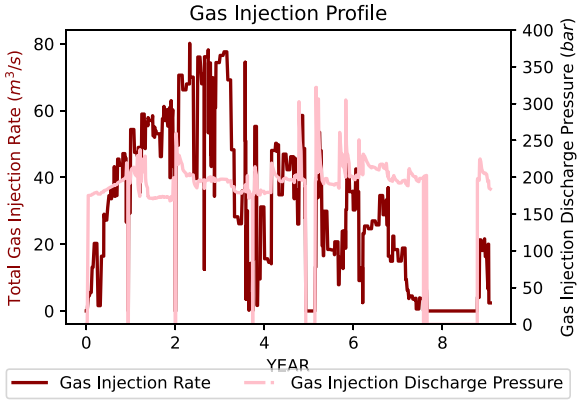

(b) Total gas injection rate and the discharge injection pressure profile from the gas injection system.

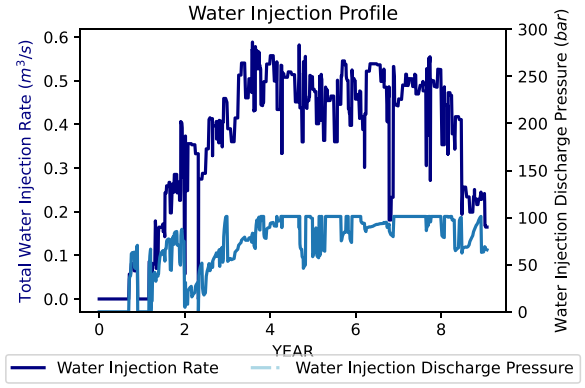

(c) Total water injection rate and the discharge injection pressure profile from the water injection system.

Fig. 6. Production and injection profile for the case study, obtained from the Norne simulation model.

2. Yearly change on the processing plant configuration, capturing the highest requirements of each system for each year.
3. Monthly change on the processing plant configuration.
4. Weekly change, which will be the most frequent change of the system configuration that we will consider in this study.

The input data stream for this case study has a daily time-step, thus a higher data density compared to the lowest frequency change on the configuration, which changes on a weekly basis. Fig. 6 shows the field profile used in the case study, showing the production profile, injection profile, and required discharge pressure profiles for nine years. Fig. 6a shows the oil, gas, and water production profile of the field, and Fig. 6b and 6c show the injection profiles for gas and water. Each injection profile corresponds to the total injection rate and required pressure for each injection well. The maximum value of these injection pressures for each gas and water injection system represents the required discharge pressure required for each injection system.

3.1. Pumping system

The pumping system head performance curve used for this study is shown in Fig. 7. This study utilizes a pumping system consisting of identical pumps, with a maximum number of stages $n = 3$ and a maximum number of trains $m = 3$. Fig. 7 shows the operational space of the pumping system with and without varying rotational speed. The left figure shows a pumping system with varying rotational speeds. The envelopes cover rotational speeds from 70% to 100% of the maximum speed. The right figure shows a more conservative pumping system, with constant rotational speed working at the maximum speed. As it is utilizing a constant speed system, it will give a single output for each rate, resulting in an inefficient pumping process and therefore higher power consumption.

The presented case study will compare the impact of different optimum configurations of the pumping system. The system with varying rotational speed is more flexible, and will therefore always yield lower power consumption than the fixed rotational speed given the same operational restrictions. However, both systems will have varying power consumption depending on the frequency of operational changes.

3.2. Compressor system

Fig. 8 shows the pressure ratio performance curves of the compressor system used in this study. It consists of identical compressors, with a maximum number of stages of $s = 3$ and a maximum number of trains of $t = 3$. The figure on the left side shows performance curves of the compressor system with varying rotational speeds of the compressor (70% to maximum rotational speed), while the right figure shows the compressor system with constant rotational speed (working at maximum speed). The gray areas in the right figure represent surge areas for the compressor system, forcing the setup to start gas re-circulation to prevent it from entering the surge area.

In the optimization conducted below, we will compare different frequencies for changing the compressor setup, i.e., changing the number of stages and trains, still having the same number of stages in each train. We will also inspect the amount of recirculated gas required in order to prevent compressor surge.

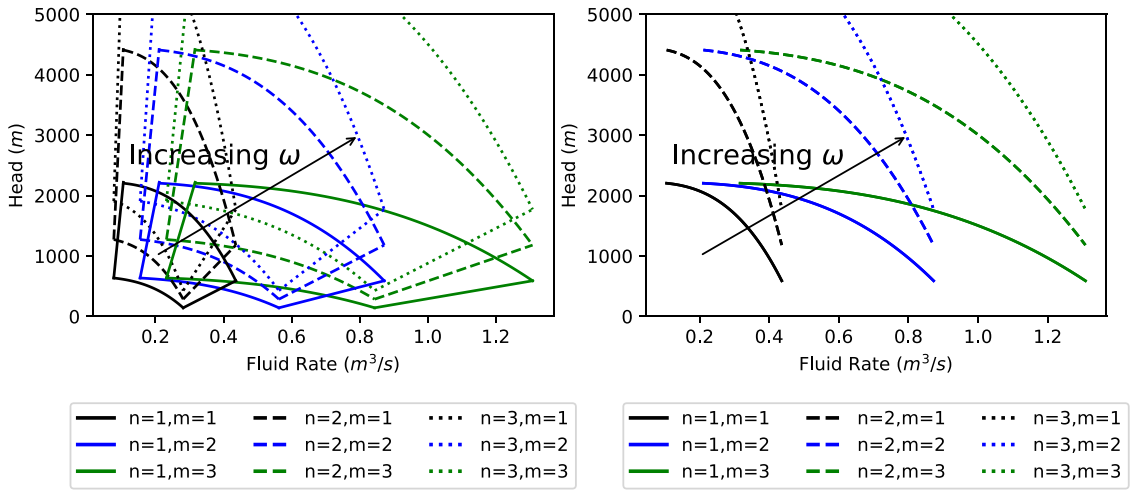

Fig. 7. Head performance curve of the water injection pumping system used in this study. The system consists of a maximum of three stages and three trains. The left figure shows a system with the possibility to change the rotational speed, while the right figure shows a more conservative pumping system working at the maximal rotational speed.

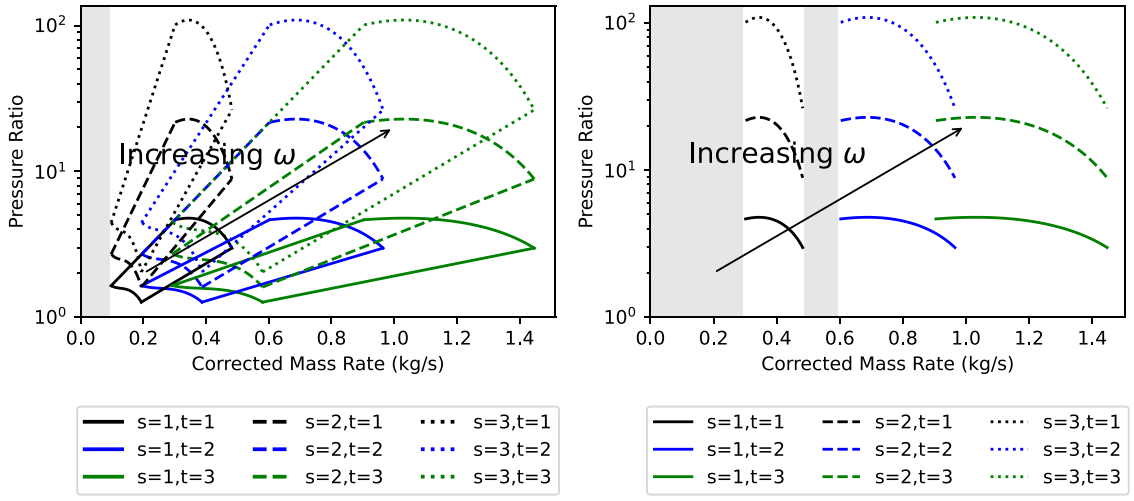

Fig. 8. Performance curve of the compressor system used in this study, showing the relation between corrected mass rate and pressure ratio. The system consists of a maximum of three stages and three trains of identical compressors. The right figure shows a compressor system with the ability to vary the rotational speed, while the left figure shows a compressor with a constant rotational speed. The gray area shows surge areas for the compressor system, triggering gas re-circulation to prevent surge.

4. Results and discussions

This section will discuss the results of the case study. We will investigate the power consumption for both varying and constant maximum rotational speeds. Further, we will discuss the impact of the frequency of the operational changes, i.e., the frequency of changing the number of trains and stages for both the pumps and compressors in the processing plant.

4.1. Water injection system results

The water injection system is injecting with a total water rate fluctuating from 0.2 SM^3/s up to 0.6 SM^3/s, with head variation up to 1000 m. Fig. 9a shows the injection profile throughout the simulated period. The plot shows that the water injection starts after shut-off for two years. We compare the results with maximum rotational speed to results where the rotational speed can be adjusted in Fig. 9b and c.

Fig. 9b shows the results for a configuration of the pumping system working on maximum rotational speed. We can see fluctuation in the number of trains (m) and the number of stages (n), as needed to provide the required total water injection rate and head. As expected, not changing the configuration for the full 9 years of injection gives the highest number of trains and stages (2 trains and 3 stages). As this setup is sub-optimal for most of the field lifetime, this setup will also consume the most power. By allowing for more frequent changes to the pump setup, e.g., yearly, monthly, or weekly, we have a significant reduction in power consumption. The highest number of trains and stages are only required for a short period in the middle of the second year, while the remainder of the field operation requires a lower number. More frequent changes to the setup will result in more optimal operation of the equipment, thus the cumulative energy consumption is lowered by higher frequency changes.

Fig. 9c shows the more flexible system which allows for changes to rotational speed. This optimization problem thus has an additional degree of freedom, which will result in even lower power consumption compared to the results for the fixed rotational speed as plotted in Fig. 9b. For a fixed setup throughout the field lifetime, the optimal solution gives a slightly lower rotational speed than the maximal rotational speed, however, the same number of pumps (3 trains and 1 stage) as in the setup that is running with maximal rotational speed. This will give a slight decrease in power consumption. Increasing the change frequency gives a further reduction in power consumption. For all frequencies, the power consumption with variation in rotational speed is reduced versus the fixed maximum speed.

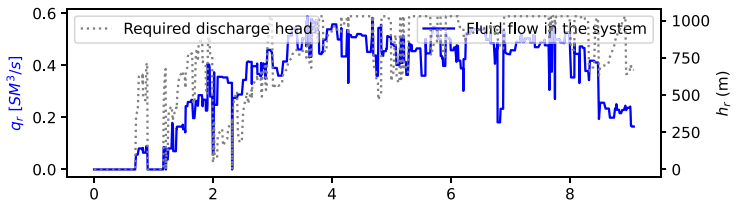

(a) Water injection flow rate (q_r) and discharge head (h_r) profile from the simulation model

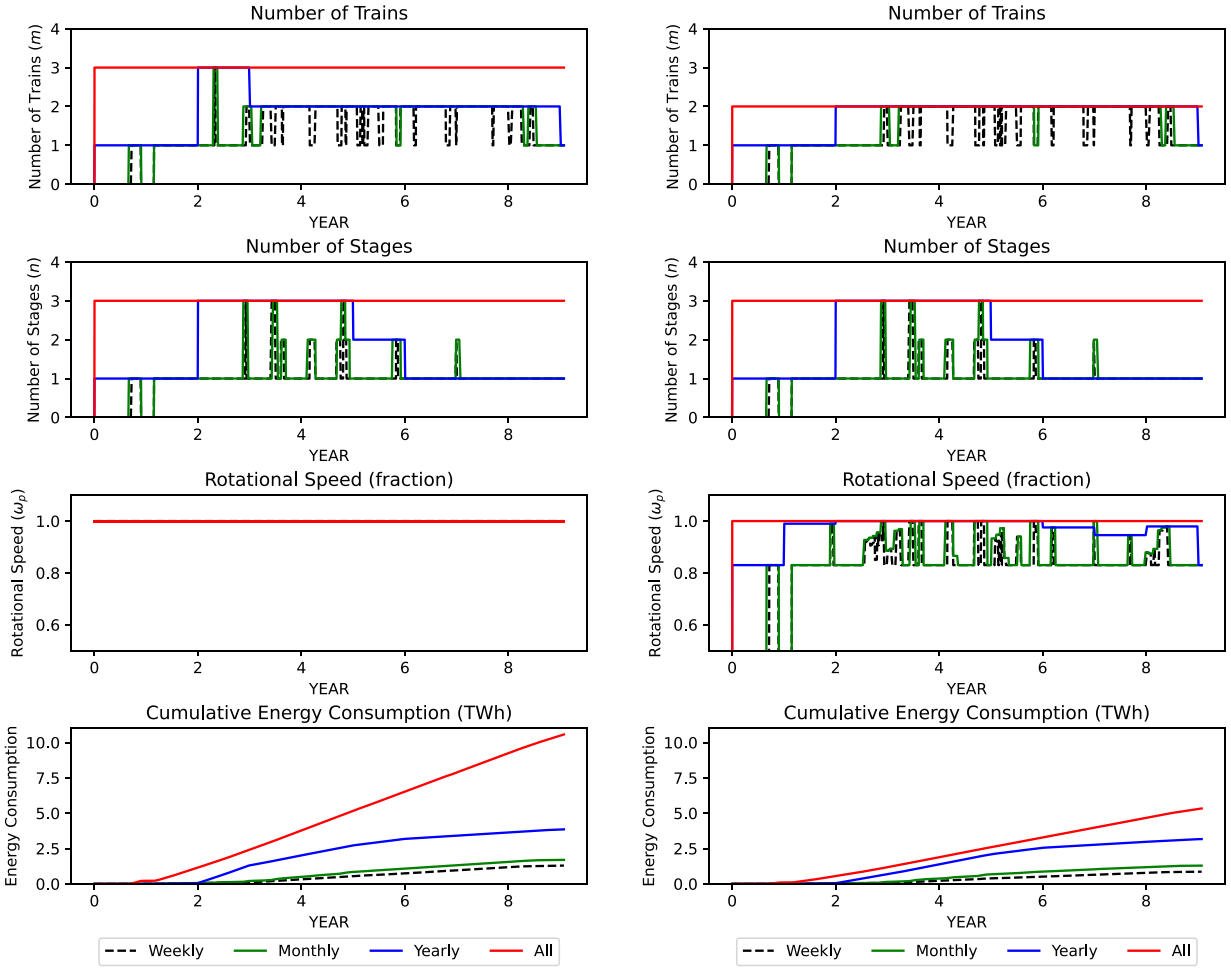

(b) The optimal pumping system configuration and its power consumption when the pumps are restricted to run at a maximum rotational speed.

(c) The optimal pumping system configuration and rotational speed, and the corresponding power consumption for the different system configurations and rotational speeds.

Fig. 9. Optimization results for the pumping system.

4.2. Gas compression system results

The gas compression system delivers gas both for gas injection back into the reservoir and for exported gas. The compressors are expected to deliver gas at a pressure corresponding to the highest of the two required pressures, i.e., the highest of the pressures needed for injection and export. The gas rate results from the produced gas, as simulated in the reservoir simulation model. Fig. 10 shows the optimization results of the gas compression system. Fig. 10a shows the corrected mass rate flowing through the compression system ($\dot{m}_r$) and the required pressure ratio (p_r). Fig. 10b shows the optimization results under the assumption of a maximal rotational speed system. Without any operational changes to the compressor system, it is required to have 3 trains and 3 stages ($s = 3, t = 3$). With more frequent operational changes the number of trains and stages can be reduced, with an associated reduction in power consumption reduction observed for the yearly and monthly frequencies. However, we see diminishing returns from more frequent changes.

Fig. 10c shows the result of a compressor where we allow for variation in rotational speed. Just as with the pumps, adding rotational speed as an additional variable in the compressor system is giving an additional reduction in energy consumption.

4.3. Discussion

The results presented above demonstrate ways to reduce the power consumption of existing processing plant equipment on offshore oil and gas platforms. This study has developed a simplified model, considering

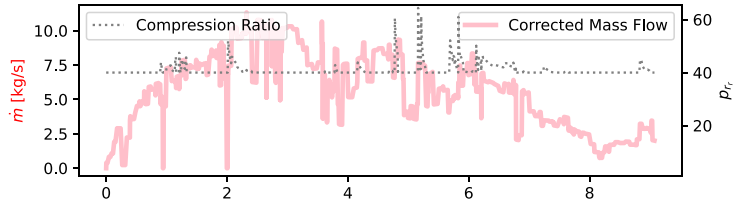

(a) Mass flow rate ($\dot{m}_r$) and pressure ratio (p_r) profile from the Norne simulation model.

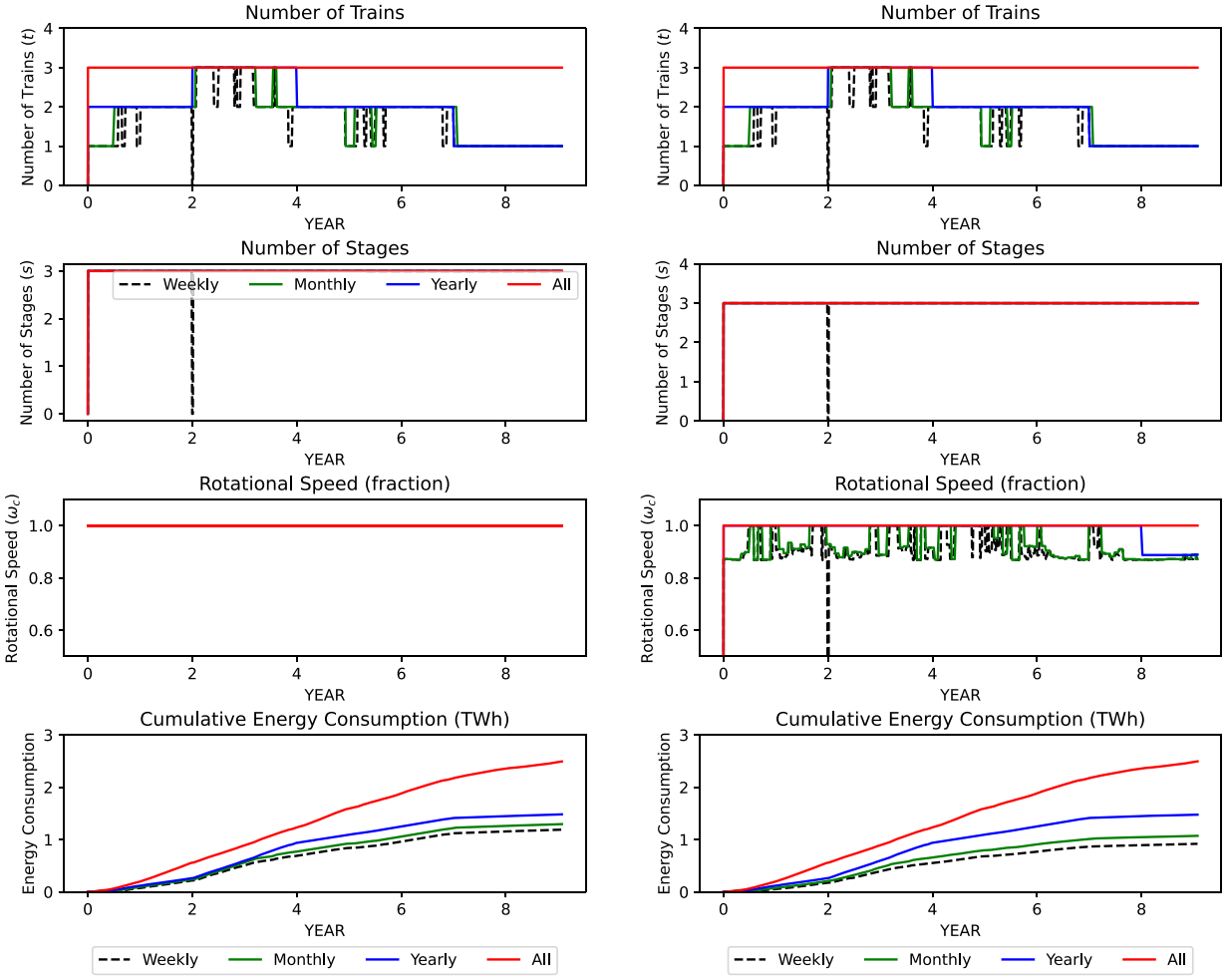

(b) The optimal gas compression system configuration when the compressors are restricted to run at a maximum rotational speed.

(c) The optimal gas compression system configuration and rotational speed, and the corresponding power consumption, for different frequencies of allowed changes to the system configuration and rotational speed.

Fig. 10. Optimization results for the gas compression system.

the performance curves of pumps and compressors and operational constraints. From our model, we observe how intervention frequency gives efficiency improvements through reduced power consumption.

One of the limitations of this study is the assumption of identical performance curves for the individual pumps and compressors. This assumption was a consequence of limited equipment data. Expanding the model to include different performance curves or adapting to settings from a producing field for the individual pumps and compressors is straightforward. However, while this will complicate the optimization problem and thereby increase the computational time for the optimization, it is still considered computationally feasible. In actual operations, future rates and pressures are unknown, and predictions deteriorate the further into the future they are. Hence the equipment setup will need to be scaled to anticipate the probable range of future rates and pressure requirements.

This study assumes steady-state operation of the processing plant equipment in each modeled time step. Paparella et al. (2013) compared compressor performance using a steady-state model to a dynamic system that was adjusting to changes in performance curves. As we are optimizing the number of compressors and pumps at each time step independently of other time steps, extending our work towards cases with frequent changes to performance curves should be straightforward.

This study highlights the correspondence between power consumption and the frequency of changes to the configuration and settings of the processing plant equipment. To investigate this correspondence further, the total energy consumption for a wide range of change

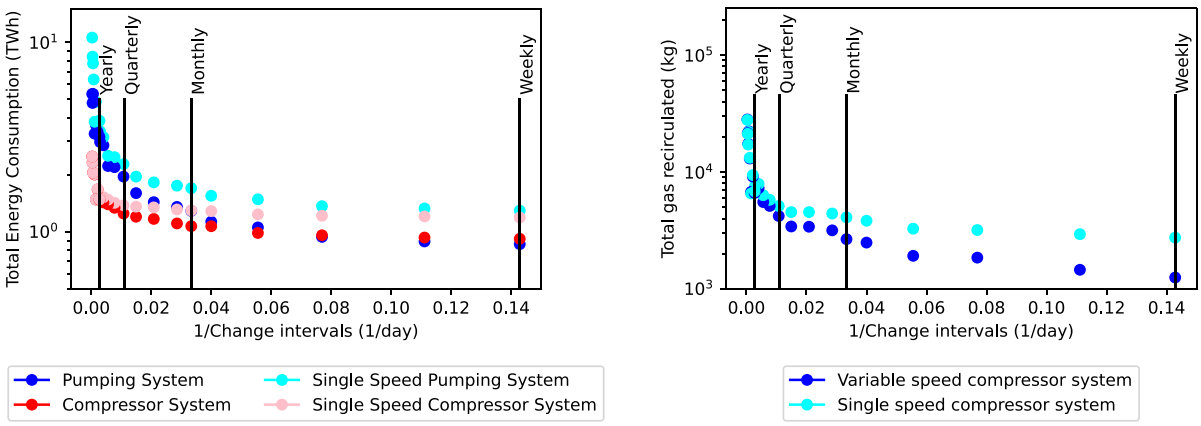

(a) Total energy consumption (in TWh) for each system. Reduction over periods of interval in changing the configurations of each system.

(b) Cumulative recirculated gas to prevent surge phenomena in each compressor versus change interval length.

Fig. 11. Plots showing the change intervals length versus (a) power consumption and (b) the amount of gas being recirculated to avoid surge.

frequencies was calculated. The results are plotted in Fig. 11. Fig. 11(a) shows a comparison between the change interval (in 1/days) and the total energy consumption of the system (in TWh). The plot indicates a steep reduction in total energy consumption for frequency changes up to quarterly changes. Further reductions in change interval have a diminishing return on reduction in power consumption.

Considering the total energy consumption of the system, we observe an increase in efficiency by increased frequency of changes to the equipment setup. Adding rotational speed as an optimization parameter to the compressor system reduces total energy consumption by 10% on average for the four tested layout-change frequencies (none, yearly, monthly, and weekly). On average for these four tested change frequencies, the pumping system has a 28% reduction in power consumption when adding rotational speed as a variable to the system. Changing the operational frequencies can reduce energy consumption more than what is obtained from adding rotation speed. Considering a fixed configuration throughout the whole production period as a baseline, a yearly change frequency reduces consumption by 41%, while cases with higher change frequency show a higher reduction. Quarterly changes yield an additional reduction of 10% compared to the yearly changes. The additional reductions diminished gradually to 7% and 5% for monthly and weekly changes, respectively. Without installing an automated system to control and change the pump and compressor setup continuously, reducing change intervals will be limited by operational limitations, e.g., costs incurred related to manual labor. There are additional inherent practical limitations that will also apply to an automated system, e.g., the start-up time of compressors and pumps. With the diminishing return from reduced change intervals, there will be an optimal interval length that balances the cost of changes with the possible reductions in power consumption. In Milosavljevic et al. (2020) the authors used model predictive control for continuous changes to the system rotational speed. The diminishing returns on reduced change frequency might indicate that the lowered power consumption achieved with an automatic controller might be limited.

Automatic control is more common for surge prevention in compressor systems, working continuously over time (Gesser et al., 2022). From our model, we obtain the amount of gas needed to be recirculated to prevent the surge in the compressors. In Fig. 11(b) we have plotted the amount of recirculated gas needed to prevent surge versus the size of the change intervals. We see that decreasing the change intervals strongly decreases the amount of recirculated gas. As with the total energy consumption, also the reduction in recirculated gas is diminishing with smaller change intervals. We also observe that increasing compressor flexibility by adding rotational speed as a variable significantly reduces the amount of gas being recirculated to prevent surge.

While this study only focuses on processing plant efficiencies and power reductions, it can be extended to be coupled with the optimization of drainage strategies. Angga et al. (2022) used similar analytical models for pumps and compressors as employed in this study, and these pump and compressor models were coupled with a reservoir simulation model to optimize the drainage strategy. The study mentioned covers an oil reservoir without associated gas. As gas compression is known to consume a significant part of the power for offshore fields, extending the mentioned study to include gas compression, as outlined in this article, would be an important contribution to understanding how drainage strategies affect power consumption, and thereby CO_2 emissions.

While this study is limited to the application of secondary recovery, i.e., water and gas injection, it is possible to expand the scope into tertiary recovery processes. This will increase the complexity of the system, but can be implemented in a simplified form similar to the approaches used in this article: Chemical injection (surfactant and polymer) uses mixing tanks and injection pumps which are similar to water pumps. Gas injection schemes (CO_2 and miscible gas) use compressor systems or multiphase pumps with similarities to the compressors used in this study.

5. Summary

This paper presents a workflow that calculates the power consumption for pumps and compressors in oil and gas processing plants. The workflows allow us to explore processing plant configurations and settings that can reduce power consumption. This paper considers two different measures to reduce power consumption during oil and gas production. The first measure is to change the equipment configuration to increase its efficiency. The second measure is adding rotational speed as an additional variable to increase flexibility to deliver the required amount at higher efficiency.

As expected, our simulations indicate that a higher frequency of changes to the processing plant configuration leads to increased efficiency and thereby lower power consumption. While there are large reductions associated with going from none to only a few operational changes to the processing plant settings, the reductions quickly tamper off. For our case study, we observed a reduction in power consumption of 41% when going from none to a yearly change in settings, while a change from monthly to weekly gave 5% reduction. Even though it is possible to achieve lower reduction with more frequent change, it may have a limited effect on increasing efficiency. In addition, there are several hindrances to a fully automatic system that can continuously change the pump and compressor setup for every change in

the input, e.g., the start-up time of compressors and pumps. Our work indicates that with respect to increased efficiency, such an automatic system working continuously changing the setup might lead to limited improvements in efficiency anyway.

This paper points towards a robust way to reduce power consumption during oil and gas production. The operational changes will increase the efficiency of the topside equipment without affecting the overall performance of the equipment, thus without affecting the subsurface drainage of the reservoir. The increased efficiency will reduce the power consumption and the fuel consumption for the power generation system in the platform, thereby reducing emissions. In addition to the improved economy due to lower fuel expenditures, the reduced CO_2 emissions will further economic benefits whenever the production is under a tax regime penalizing CO_2 emissions.

CRediT authorship contribution statement

Handita Reksi Dwitantra Sutoyo: Conceptualization, Methodology, Investigation, Writing – original draft, Visualization. **I Gusti Agung Gede Angga:** Formulation, Investigation, Writing – review & editing. **Heiner Schümann:** Supervision, Project administration, Funding acquisition, Writing – review & editing. **Carl Fredrik Berg:** Formal analysis, Writing – original draft, Supervision.

Declaration of competing interest

The authors declare that they have no known competing financial interests or personal relationships that could have appeared to influence the work reported in this paper.

Data availability

No data was used for the research described in the article

Acknowledgments

The first author, Handita Reksi Dwitantra Sutoyo, and the second author, I Gusti Agung Gede Angga are supported by the Research Council of Norway through its Research Centers for Petroleum (PETROSENTRE) program, project number 296207, Low Emission. The author would like to thank Associate Professor Milan Stanko from Department of Geoscience and Petroleum, NTNU, for valuable inputs and discussions for the research.

Appendix A. Calculation

This section will elaborate the detailed calculation and equations used specifically for this study with Appendix A.1 for the pumping system conversion and A.2 for the compressor system.

A.1. Water injection system

$$p_{op} = p_{wi}(t) \tag{17}$$

$$p_{ip} = 1 \times 10^5 \text{ Pa} \tag{18}$$

$$h_r = \frac{p_{op} - p_{ip}}{\rho_f \cdot g} \tag{19}$$

$$q_r = q_{wi} \tag{20}$$

In this paper, we assume ρ_f (water density) is $1000\,\text{kg/m}^3$ and g (gravity acceleration) is $9.81\,\text{m/s}^2$.

Table 2
Constants for pump head and efficiency performance.

Parameter	Value
a_0	1.8231×10^3
a_1	-5.641×10^1
a_2	6.409×10^1
a_3	2.061×10^2
a_4	1.712×10^2
a_5	-1.868×10^2
$\bar{q}$	1.593×10^{-1}
ω_q	7.068×10^2
ω_2	1.942×10^7
ω_3	8.672×10^{10}
q_3	7.922×10^{-3}
σ_q	8.964×10^{-2}
$\sigma_{\omega q}$	4.196×10^1
$\sigma_{\omega 2}$	3.681×10^1
$\sigma_{\omega 3}$	2.407×10^1
σ_{q3}	9.304×10^{-3}
b_0	1×10^{-10}
b_1	9.641
b_2	-3.812×10^1
b_3	5.741×10^{-3}
b_4	-1.629×10^{-7}

A.2. Gas compression system

$$p_{oc} = \max[p_{gi}(t), p_d(t)] \tag{21}$$

$$q_{gd} = \max[q_{gp}(t), q_{gi}(t)] \tag{22}$$

$$p_{ic} = p_p(t) \tag{23}$$

$$p_{r_r} = \frac{p_{oc}}{p_{ic}} \tag{24}$$

$$\dot{m}_r = \frac{q_{gd}}{\rho_g\big|_{p_{ic},T_{ic}}} \tag{25}$$

Appendix B. Pump performance curve

The pump performance is described by the following two relationships, adapted from (Angga et al., 2022).

$$h_p = a_0 + a_1 \cdot \left(\frac{q_p - \bar{q}}{\sigma_q}\right) + a_2 \cdot \left(\frac{\omega_p \cdot q_p - \bar{\omega_q}}{\sigma_{\omega q}}\right) + a_3 \cdot \left(\frac{(\omega_p)^2 - \bar{\omega_2}}{\sigma_{\omega 2}}\right) + a_4 \cdot \left(\frac{(\omega_p)^3 - \bar{\omega_3}}{\sigma_{\omega 3}}\right) + a_5 \cdot \left(\frac{(q_p)^3 - \bar{q_3}}{\sigma_{q3}}\right) \tag{26}$$

$$\eta_p = b_0 + b_1 \cdot q_p + b_2 \cdot q_p^2 + b_3 \cdot \omega_p \cdot q_p^2 + b_4 \cdot (\omega_p)^2 \cdot q_p \tag{27}$$

Constants for the pump performance curves are pump dependent. The constants used in this study are provided in Table 2.

Appendix C. Compressor performance curve

The compressor performance is described by these relationship, adapted from (Jiang et al., 2019).

$$p_r = g_0 + g_1 \cdot \frac{\omega_c}{\omega_0} \cdot \frac{\dot{m}_c}{m_0} + g_2 \cdot \dot{m}_c^2 + g_3 \cdot \frac{\omega_c}{\omega_0} \cdot \left(\frac{\dot{m}_c}{m_0}\right)^2 + g_4 \cdot \left(\frac{\omega_c}{\omega_0}\right)^2 + g_5 \cdot \frac{\left(\frac{\omega_c}{\omega_0}\right)^3}{\left(\frac{\dot{m}_c}{m_0}\right)} \tag{28}$$

$$\eta_s = f_0 \cdot \left(\frac{\omega_c}{\omega_0}\right) + f_1 \cdot \left(\frac{\omega_c}{\omega_0}\right)^2 + f_2 \cdot \left(\frac{\omega_c}{\omega_0}\right)^3 + f_3 \cdot \frac{\left(\frac{\omega_c}{\omega_0}\right)^{f_4}}{\left(\frac{\dot{m}_c}{m_0}\right)} + f_5 \cdot \frac{\left(\frac{\omega_c}{\omega_0}\right)^{f_6}}{\left(\frac{\dot{m}_c}{m_0}\right)} + f_7 \cdot \left(\frac{\omega_c}{\omega_0}\right)^{f_8} \cdot \frac{\dot{m}_c}{m_0} \tag{29}$$

Constants for the pump performance curve is provided in Table 3.

Table 3
Constants for pump head and efficiency performance.

Parameter	Value
g_0	1.045
g_1	2.412×10^{2}
g_2	-1.086×10^{3}
g_3	1.868×10^{2}
g_4	-1.885×10^{1}
g_5	5.804×10^{-1}
f_0	8.06×10^{1}
f_1	5.011×10^{1}
f_2	-1.548×10^{-1}
f_3	4.27×10^{-9}
f_4	-1.434×10^{1}
f_5	-7.023×10^{-1}
f_6	2.918×10^{1}
f_7	-5.164×10^{1}
f_8	-2.334×10^{-2}
ω_0	1.390×10^{5}
m_0	2.5

References

Aguilera, R.F., 2021. Effects of technological progress and external costs on upstream petroleum supply. J. Pet. Sci. Eng. 202, 108522. http://dx.doi.org/10.1016/j.petrol.2021.108522, URL: https://www.sciencedirect.com/science/article/pii/S0920410521001819.

Ahonen, T., Pöyhönen, S., Siimesjärvi, J., Tolvanen, J., 2019. Graphic determination of available energy-saving potential in a reservoir pumping application with variable-speed operation. Energy Effic. 12 (5), 1041–1051. http://dx.doi.org/10.1007/s12053-018-9712-y.

Al-Fattah, S.M., 2020. Non-OPEC conventional oil: Production decline, supply outlook and key implications. J. Pet. Sci. Eng. 189, 107049. http://dx.doi.org/10.1016/j.petrol.2020.107049, URL: https://www.sciencedirect.com/science/article/pii/S0920410520301431.

Angga, I.G.A.G., Bellout, M., Kristoffersen, B.S., Bergmo, P.E.S., Slotte, P.A., Berg, C.F., 2022. Effect of CO2 tax on energy use in oil production: waterflooding optimization under different emission costs. SN Appl. Sci. 4 (11), 313. http://dx.doi.org/10.1007/s42452-022-05197-4, URL: https://link.springer.com/10.1007/s42452-022-05197-4.

Arun Shankar, V.K., Umashankar, S., Paramasivam, S., Hanigovszki, N., 2016. A comprehensive review on energy efficiency enhancement initiatives in centrifugal pumping system. Appl. Energy 181, 495–513. http://dx.doi.org/10.1016/j.apenergy.2016.08.070, URL: https://www.sciencedirect.com/science/article/pii/S0306261916311576.

Bothamley, M., 2004. Offshore Processing Options for Oil Platforms. OnePetro, http://dx.doi.org/10.2118/90325-MS, URL: https://onepetro.org/SPEATCE/proceedings/04ATCE/All-04ATCE/SPE-90325-MS/71620.

Cortinovis, A., Mercangöz, M., Zovadelli, M., Pareschi, D., De Marco, A., Bittanti, S., 2016. Online performance tracking and load sharing optimization for parallel operation of gas compressors. Comput. Chem. Eng. 88, 145–156. http://dx.doi.org/10.1016/j.compchemeng.2016.01.012, URL: https://www.sciencedirect.com/science/article/pii/S0098135416300035.

da Costa Bortoni, E., de Almeida, R.A., Viana, A.N.C., 2008. Optimization of parallel variable-speed-driven centrifugal pumps operation. Energy Effic. 1 (3), 167–173. http://dx.doi.org/10.1007/s12053-008-9010-1.

Gesser, R.S., Sartori, R., Damo, T.P., Vettorazzo, C.M., Becker, L.B., Lima, D.M., de Lima, M.L., Ribeiro, L.D., Campos, M.C.M.M., Normey-Rico, J.E., 2022. Advanced control applied to a gas compression system of an offshore platform: From modeling to related system infrastructure. J. Pet. Sci. Eng. 208, 109428. http://dx.doi.org/10.1016/j.petrol.2021.109428, URL: https://www.sciencedirect.com/science/article/pii/S0920410521010731.

IEA, 2021a. Global energy review 2021 – analysis. URL: https://www.iea.org/reports/global-energy-review-2021.

IEA, 2021b. World energy outlook 2021 – analysis. URL: https://www.iea.org/reports/world-energy-outlook-2021.

IEA, 2022. Oil and natural gas supply. URL: https://www.iea.org/reports/oil-and-natural-gas-supply.

Jiang, H., Dong, S., Liu, Z., He, Y., Ai, F., 2019. Performance prediction of the centrifugal compressor based on a limited number of sample data. Math. Probl. Eng. 2019, e5954128. http://dx.doi.org/10.1155/2019/5954128, URL: https://www.hindawi.com/journals/mpe/2019/5954128/.

Kloster, P., 1999. Energy Optimization on Offshore Installations with Emphasis on Offshore Combined Cycle Plants. OnePetro, http://dx.doi.org/10.2118/56964-MS, URL: https://onepetro.org/SPEOE/proceedings/99OE/All-99OE/SPE-56964-MS/60456.

Kloster, P., 2000. Reduction of Emissions to Air through Energy Optimisation on Offshore Installations. OnePetro, http://dx.doi.org/10.2118/61651-MS, URL: https://onepetro.org/SPEHSE/proceedings/00HSE/All-00HSE/SPE-61651-MS/131737.

Kurz, R., Brun, K., 2017. Process control for compression systems. J. Eng. Gas Turbines Power 140 (2), http://dx.doi.org/10.1115/1.4037723.

Leufvén, O., Eriksson, L., 2013. A surge and choke capable compressor flow model—Validation and extrapolation capability. Control Eng. Pract. 21 (12), 1871–1883. http://dx.doi.org/10.1016/j.conengprac.2013.07.005, URL: https://www.sciencedirect.com/science/article/pii/S0967066113001354.

Li, X., Cui, T., Huang, K., Ma, X., 2021. Optimization of load sharing for parallel compressors using a novel hybrid intelligent algorithm. Energy Sci. Eng. 9 (3), 330–342. http://dx.doi.org/10.1002/ese3.821, URL: https://onlinelibrary.wiley.com/doi/abs/10.1002/ese3.821.

McKenna, R., D'Andrea, M., González, M.G., 2021. Analysing long-term opportunities for offshore energy system integration in the Danish North Sea. Adv. Appl. Energy 4, 100067. http://dx.doi.org/10.1016/j.adapen.2021.100067, URL: https://www.sciencedirect.com/science/article/pii/S2666792421000597.

Milosavljevic, P., Marchetti, A.G., Cortinovis, A., Faulwasser, T., Mercangöz, M., Bonvin, D., 2020. Real-time optimization of load sharing for gas compressors in the presence of uncertainty. Appl. Energy 272, 114883. http://dx.doi.org/10.1016/j.apenergy.2020.114883, URL: https://www.sciencedirect.com/science/article/pii/S0306261920303950.

Nguyen, T.V., Jacyno, T., Breuhaus, P., Voldsund, M., Elmegaard, B., 2014. Thermodynamic analysis of an upstream petroleum plant operated on a mature field. Energy 68, 454–469. http://dx.doi.org/10.1016/j.energy.2014.02.040, URL: https://www.sciencedirect.com/science/article/pii/S0360544214001741.

Nguyen, T.V., de Oliveira Júnior, S., 2018. Life performance of oil and gas platforms for various production profiles and feed compositions. Energy 161, 583–594. http://dx.doi.org/10.1016/j.energy.2018.07.121, URL: https://www.sciencedirect.com/science/article/pii/S036054421831418X.

Nguyen, T.V., Pierobon, L., Elmegaard, B., Haglind, F., Breuhaus, P., Voldsund, M., 2013. Exergetic assessment of energy systems on North Sea oil and gas platforms. Energy 62, 23–36. http://dx.doi.org/10.1016/j.energy.2013.03.011, URL: https://www.sciencedirect.com/science/article/pii/S0360544213001874.

Nguyen, T.V., Voldsund, M., Breuhaus, P., Elmegaard, B., 2016. Energy efficiency measures for offshore oil and gas platforms. Energy 117, 325–340. http://dx.doi.org/10.1016/j.energy.2016.03.061, URL: https://www.sciencedirect.com/science/article/pii/S036054421630305X.

NPD, 2021. Emissions to air. URL: https://www.norskpetroleum.no/en/environment-and-technology/emissions-to-air/.

OPM, 2022. Norne benchmark case. original-date: 2019-05-09T11:35:01Z. URL: https://github.com/OPM/opm-data/tree/master/norne.

Paparella, F., Domínguez, L., Cortinovis, A., Mercangöz, M., Pareschi, D., Bittanti, S., 2013. Load sharing optimization of parallel compressors. In: 2013 European Control Conference. ECC, pp. 4059–4064. http://dx.doi.org/10.23919/ECC.2013.6669697.

Riboldi, L., Nord, L.O., 2017. Concepts for lifetime efficient supply of power and heat to offshore installations in the North Sea. Energy Convers. Manage. 148, 860–875. http://dx.doi.org/10.1016/j.enconman.2017.06.048, URL: https://www.sciencedirect.com/science/article/pii/S0196890417305940.

Roussanaly, S., Aasen, A., Anantharaman, R., Danielsen, B., Jakobsen, J., Heme-De-Lacotte, L., Neji, G., Sødal, A., Wahl, P.E., Vrana, T.K., Dreux, R., 2019. Offshore power generation with carbon capture and storage to decarbonise mainland electricity and offshore oil and gas installations: A techno-economic analysis. Appl. Energy 233–234, 478–494. http://dx.doi.org/10.1016/j.apenergy.2018.10.020, URL: https://www.sciencedirect.com/science/article/pii/S0306261918315745.

Sentralbyrå, S., 2021. Utslipp til luft. Stat. Sentralbyrå-Stat. Norway URL: https://www.ssb.no/natur-og-miljo/forurensning-og-klima/statistikk/utslipp-til-luft.

Shen, H., Zhang, C., Zhang, J., Yang, B., Jia, B., 2020. Applicable and comparative research of compressor mass flow rate and isentropic efficiency empirical models to marine large-scale compressor. Energies 13 (1), 47. http://dx.doi.org/10.3390/en13010047, URL: https://www.mdpi.com/1996-1073/13/1/47.

Stewart, M., 2019a. 3 - Centrifugal pumps. In: Stewart, M. (Ed.), Surface Production Operations. Gulf Professional Publishing, Boston, pp. 61–309. http://dx.doi.org/10.1016/B978-0-12-809895-0.00003-X, URL: https://www.sciencedirect.com/science/article/pii/B978012809895000003X.

Stewart, M., 2019b. 7 - Compressor fundamentals. In: Stewart, M. (Ed.), Surface Production Operations. Gulf Professional Publishing, Boston, pp. 457–525. http://dx.doi.org/10.1016/B978-0-12-809895-0.00007-7, URL: https://www.sciencedirect.com/science/article/pii/B9780128098950000077.

Viholainen, J., Tamminen, J., Ahonen, T., Ahola, J., Vakkilainen, E., Soukka, R., 2013. Energy-efficient control strategy for variable speed-driven parallel pumping systems. Energy Effic. 6 (3), 495–509.

Voldsund, M., Ertesvåg, I.S., He, W., Kjelstrup, S., 2013. Exergy analysis of the oil and gas processing on a North Sea oil platform a real production day. Energy 55, 716–727. http://dx.doi.org/10.1016/j.energy.2013.02.038, URL: https://www.sciencedirect.com/science/article/pii/S0360544213001527.

Yazar, I., Yavuz, H.S., Yavuz, A.A., 2017. Comparison of various regression models for predicting compressor and turbine performance parameters. Energy 140, 1398–1406. http://dx.doi.org/10.1016/j.energy.2017.05.061, URL: https://www.sciencedirect.com/science/article/pii/S0360544217308174.

Zhong, M., Bazilian, M.D., 2018. Contours of the energy transition: Investment by international oil and gas companies in renewable energy. Electr. J. 31 (1), 82–91. http://dx.doi.org/10.1016/j.tej.2018.01.001, URL: https://www.sciencedirect.com/science/article/pii/S1040619017303561.